Controlled Elaboration and Magnetic Properties of Submicrometric Cobalt Fibers

Amel Dakhlaoui,*,†,‡ Leila S. Smiri,† Gerard Babadjian,§ Frédéric Schoenstein,‡ Philippe Molinié,∥,⊥ and Noureddine Jouini‡

Unité de recherche 99/UR12-30, Département de Chimie, Faculté des Sciences de Bizerte, 7021 Jarzouna, Tunisie, IUT Saint-Denis, Université Paris 13, Place du 8 mai 1945; 93400 Saint-Denis, France, Laboratoire des Propriétés Mécaniques et Thermodynamiques des Matériaux, LPMTM, CNRS UPR 9001 Université Paris XIII, 99 Avenue J.B. Clément, 93430 Villetaneuse; France, and Institut Jean Rouxel des Matériaux, 2 Chemin de la Houssinière, F-44072 Nantes Cedex, France

Received: April 28, 2008; Revised Manuscript Received: June 26, 2008

Hexagonal close-packed cobalt fibers with a narrow size distribution and a submicrometric diameter have been successfully synthesized using a modified polyol process in the presence of an applied magnetic field of 500 Oe. The X-ray diffraction (XRD) and the scanning electron microscopy characterization showed that the structure, size, morphology, and dispersion of the as-prepared fibers were widely influenced by the synthesis parameters (hydrolysis ratio, reactant concentration, reaction temperature, and time). The selected area electron diffraction pattern revealed that the as-prepared fibers are polycrystalline. Magnetic measurements on cobalt samples showed enhancement of their ferromagnetic properties, which may be attributed to their anisotropic shape. Irreversibility in the zero-field-cooling and field-cooling measurements was observed and could be interpreted in terms of the unblocking of magnetization of small-domain particles and domain wall depinning of larger multidomain particles.

1. Introduction

Magnetic nanoparticles have attracted increasing interest among researchers because of their promising applications in various fields such as high-density magnetic recording media, ferrofluids, magnetic refrigeration systems, biomedicine, and catalysts.[1−6] Cobalt, in particular, is one of the most important ferromagnetic materials for its interesting size- and shape-dependent magnetic, electronic, and catalytic properties.[1,7] Therefore, great efforts have been focused on the elaboration of cobalt with controlled morphology and structure by means of different physical and chemical methods. When studying cobalt nanowires obtained by electro-deposition, Henry[8] and Paulus[9] noticed that crystal anisotropy either concurs with shape anisotropy in maintaining the Co magnetization aligned parallel or is perpendicular to the axis of the wire. These distinctive anisotropic magnetic properties make Co nanowires a potential candidate for perpendicular magnetic recording. Moreover, the electronic, photonic, and energy transfer between one-dimensional (1D) nanoparticle assemblies make them important for the production of novel devices and for the understanding of fundamental phenomena at the nanometer-scale.[10−12] Thus, there has been tremendous experimental research on the 1D cobalt assemblies involving the interaction between the synthesis conditions, the structure, and the magnetic properties. Hence, different experiments using linear or quasilinear templates (polyeletctrolytes, biomolecules, tubes, polycarbonate membranes, etc.), surfactants, or self-organization of magnetic particles by means of a magnetic field were used to induce the anisotropic growth of the particles. Via a surfactant-assisted hydrothermal method, Zhang and co-workers[1] have elaborated magnetic hexagonal close-packed (hcp) cobalt chains of 5−10 μm in diameter and 100−300 μm in length at 100 °C starting from cobalt chloride in the presence of the sodium dodecylsulfate (SDS) surfactant and the sodium tartrate complex reagent. The surfactant made it possible to control the formation of cobalt nanostructures since it selectively adsorbes on crystallographic facets of the growing crystal and determines their growth rates. These pieces of work have also shown that the reaction conditions, including the reaction temperature and the alkalinity of the solution, were also key parameters influencing the formation of cobalt chains and their magnetic characteristics such as magnetization saturation and coercivity (M_s, H_c). The Wang group[13] has investigated the effect of a static magnetic field on the morphology of cobalt nanowires prepared by γ-irradiation of $CoCl_2$, CH_3COONa, and isopropyl alcohol solution. It has been noted that the extrastrong external field (1.1 T) has significantly influenced the aggregation ways of the cobalt particles produced and cobalt crystallization. Wu et al.[14] have also elaborated cobalt fibers using an external magnetic field to induce anisotropic growth of the particles: a metal salt, namely, cobalt acetate hydrate, is reduced in a boiling ethylene glycol liquid. As the reaction took place, a constant magnetic field was applied to cause the attachment of the fine spherical metal particles. Although, this group succeeded in obtaining cobalt fibers, the diameter still remains micrometric (about 1.5 μm), and the reaction temperature and time are relatively high, which is energy consuming. Furthermore, the magnetic field is applied after the reaction took place so that the metal particles, already formed in the reactional medium, attach to each other likely by dipole−dipole and van der Waals interactions. In all these previously cited studies, the synthesized Co fibers present a micrometric diameter and/or a mixture of hcp and face-centered cubic (fcc) phases. So it is still difficult to control either

* Corresponding author phone: +33 149 40 34 96; fax: +33 149 40 39 38; e-mail: dakhlaoui_amel@yahoo.fr.
† Faculté des Sciences de Bizerte.
‡ Laboratoire des Propriétés Mécaniques et Thermodynamiques des Matériaux.
§ IUT Saint-Denis.
∥ Philippe Molinié is deceased as of April 27, 2008.
⊥ Institut Jean Rouxel des Matériaux.

10.1021/jp804461s CCC: $40.75
Published on Web 08/21/2008

TABLE 1: Conditions for Synthesis of Co Fibers and the Most Attractive Results

sample	b^a	r^b	temperature (°C)	reaction time (h)	observation of the powder	phase
Co_1	**1**	14	90	2	a mixture of fibers and isotropic particles	fcc and hcp
Co_2	**2**	14	90	2	a mixture of fibers and isotropic particles	fcc and hcp
Co_3	**3**	**14**	90	2	homogenous preparation: powder contains only submicrometric fibers	hcp
Co_4	3	**10**	90	2	a mixture of fibers and isotropic particles	fcc and hcp
Co_5	3	**16**	90	2	a mixture of fibers and isotropic particles	fcc and hcp
Co_6	3	14	**78**	**5**	homogenous preparation: powder contains only micrometric fibers	hcp

[a] The basic ratio. [b] The reducing ratio.

the structure, to prepare the pure hexagonal phase, or the diameter, to obtain stable nanometric or submicrometric Co fibers.

Here, we report on the fabrication of cobalt fibers with a very well-controlled structure (hcp or hcp and fcc) and diameter in the submicrometric range using a modified polyol process. The main modifications brought to the well-known polyol process initiated by Fiévet et al.[15] are (i) the use of a strong reducing agent, (ii) the use of a nucleating agent, and (iii) the presence of an applied magnetic field during both nucleation and growth steps. The influence of different synthesis parameters (amount of NaOH and hydrazine, temperature, and nucleating agent) on the formation of these cobalt fibers and their structure (hcp or hcp and fcc) has been studied in detail. The static magnetic properties of the micrometric and submicrometric as-prepared Co fibers have also been studied: their magnetic characterization has been carried out by hysteresis loop measurements at 5 and 300 K, and the temperature dependence of their magnetization has been studied by means of the zero-field-cooling and field-cooling (ZFC/FC) curves between 5 and 380 K.

2. Experiment Methods

2.1. Synthesis of Cobalt Fibers. In a typical experiment, 0.064 g of cobalt(II) acetate tetrahydrate (99%, Aldrich) was dissolved in 7.2 mL of ethylene glycol, then mixed with 0.26−0.77 mL of a 1 M sodium hydroxide solution, and uniformly stirred at room temperature. Subsequently, 0.194−0.311 mL of hydrazine hydroxide solution (80%) was added to the mixture and ultrasonically agitated for about a half-hour. The reactor containing the obtained pink slurry was then placed in an oil-bath previously heated at the desired temperature, and a magnetic field of about 500 oersted was immediately applied. The reaction was allowed to proceed from 2 to 8 h. At the end of the reaction, the magnet was removed, the suspension was cooled to room temperature, and the gray-colored cobalt powder was separated from the solution by centrifugation, washed with alcohol and acetone several times, and then dried in an oven at 50 °C. Reaction parameters such as temperature and time of reduction, precursor concentration, basic ratio (b = [NaOH]/[Co]) and reducing ratio (r = [N_2H_5OH]/[Co]) were varied to control the size, the shape, and the dispersion state of the synthesized cobalt fibers.

2.2. Characterization Techniques. Characterization of the powder necessitates different techniques. The X-ray diffraction patterns were obtained using an INEL diffractometer with a cobalt anticathode (λ = 1.7809 Å). Analysis of the morphology of the samples was carried out on a LEICH 440 Scanning electron microscope (SEM). The investigations were carried out at room temperature applying a voltage of 15 kV. The free working distance (FWD) varies from 9 to 15 mm. Transmission electron microscopy (TEM) and selected area electron diffraction patterns (SAED) were taken with a JEOL-2011 TEM operating at an accelerating voltage of 200 kV. The thermal decomposition behavior of the as-synthesized fibers was examined by means of thermo-gravimetric analysis (TGA) using a SETSYS Evolution-1750 SETARAM instrument in Ar atmosphere at a heating rate of 10 K min^{-1}. A superconducting quantum interference device (SQUID) magnetometer was used to measure the magnetic properties of Co fibers. The hysteresis loops were recorded at 5 and 300 K. The ZFC/FC curves were registered between 5 and 380 K at an applied magnetic field of 200 Oe. To obtain the ZFC curve, the sample was first cooled with no field to 5 K and then heated under an applied magnetic field of 200 Oe while the net magnetization of the sample is recorded. The FC curve was recorded after the ZFC experiment. The procedure is the same except that the sample was cooled with the presence of the magnetic field.

3. Results and Discussion

Magnetic cobalt fibers have been earlier prepared by the polyol process with ethylene glycol that acts both as solvent and as reducing agent.[14] Reactions have been conducted at the boiling temperature of polyol (about 197 °C) for about eight hours. The cobalt fibers produced have micrometric diameters. In our study, the addition of the hydrazine hydroxide, as reducing agent, to the cobaltous suspensions has allowed reduction to be performed at a lower temperature; the formation of cobalt powder might be completed within 5 min at 90 °C and within 5 h at 78 °C. Therefore, for almost all the experiments, the temperature of the oil-bath was fixed at 90 °C, and the reaction was allowed to proceed for 2 h so that reduction was undoubtedly achieved. The most attractive results with synthesis conditions are reported in Table 1.

3.1. Effect of NaOH and Hydrazine Amounts. During the course of the reactions the basic ratio b was varied from 1 to 3 while fixing the reaction time to 2 h, the reducing ratio r to 14, and the precursor concentration to 0.032 M. It was found that for $b \leq 2$ (samples Co_1 and Co_2), the powder obtained is a mixture of cobalt fibers and isotropic particles (Figure 1a). At the basic ratio of 3 (sample Co_3), desirable results are obtained: SEM micrographs showed that the powder contains only nonagglomerated cobalt fibers 0.3 μm in diameter and about 40 μm in length (Figure 1b). The X-ray diffraction study shows that the powder obtained in the first case ($b \leq 2$), is a mixture of hexagonal (hcp) and cubic (fcc) phases (Figure 2a), whereas the fibers obtained in the second case ($b = 3$), have a hexagonal structure (hcp) (Figure 2b). No impurities could be detected in the pattern, which implies that the pure hcp Co phase could be obtained under these synthesis conditions. To further investigate if obtaining the pure hcp phase is related to the presence of exclusive fibers in the powder, a sample has been prepared under similar conditions with a basic ratio of 3 but without the presence of the external magnetic field. Its X-ray pattern shows the presence of the hexagonal (hcp) and cubic (fcc) phases, and its SEM micrograph reveals that the powder is constituted only by isolated particles. This illustrates that the pure hexagonal phase is favored when the growth mechanism leads to cobalt fibers instead of isolated isotropic particles. Thus, besides the

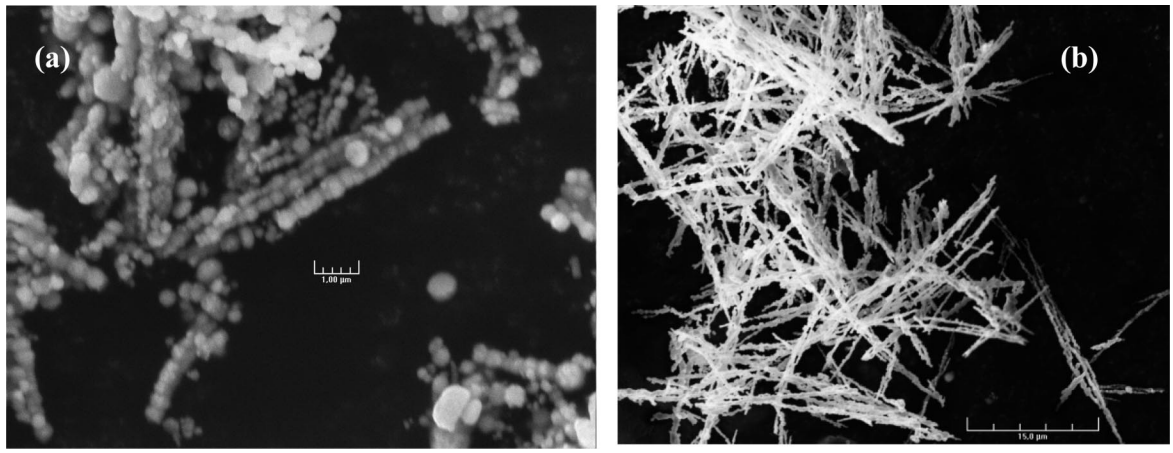

Figure 1. SEM micrographs of cobalt powder obtained at a basic ratio of 2 (a) and 3 (b).

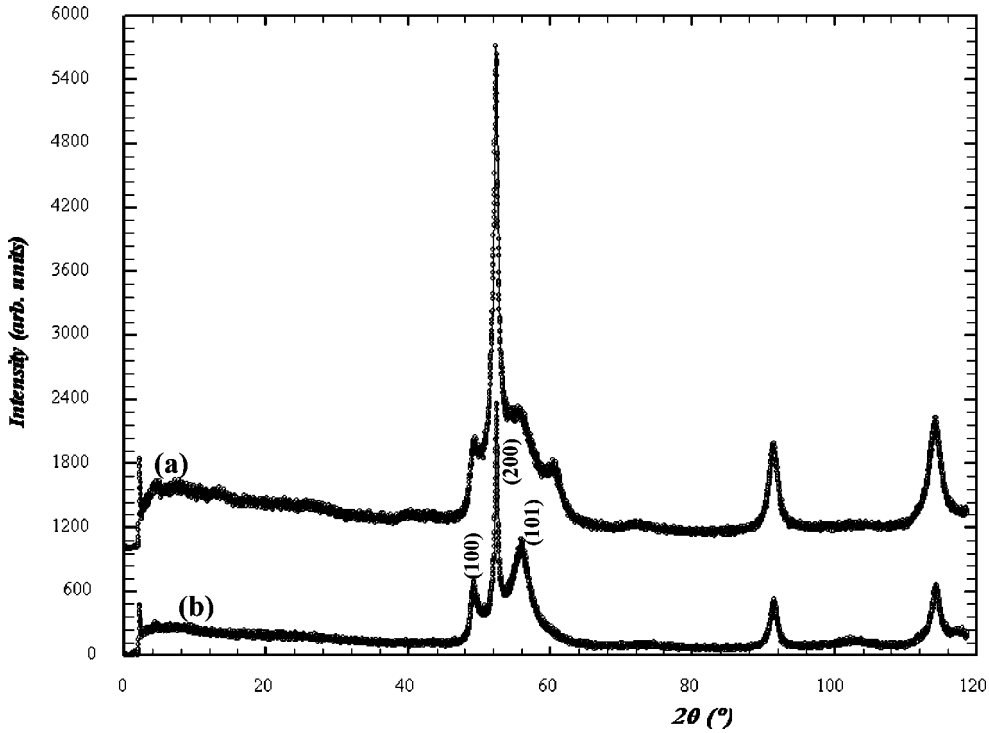

Figure 2. XRD patterns of cobalt fibers prepared with a basic ratio of 2 (a) and 3 (b).

anisotropic shape of these cobalt fibers, they present a high magneto-crystalline anisotropy since they crystallize as an hcp phase, which is of special interest for a range of applications, namely, in the field of permanent magnets.[1,16]

The study of the effect of the reducing ratio (samples Co_3, Co_4, and Co_5) highlights its influence on the structure of cobalt fibers and morphology of particles. In fact, when $r < 12$ or $r > 14$, the powder obtained is a mixture of isotropic and anisotropic cobalt particles, whereas at a reducing ratio in the 12−14 range, the powder is formed by homogeneous cobalt fibers.

According to these results, the basic and reducing ratios were fixed at 3 and 14, respectively, during the reaction experiments.

3.2. Effect of the Temperature. Because the temperature was supposed to be responsible for the reaction rate to form cobalt particles, reductions were performed at 90 and 78 °C while fixing the precursor concentration at 0.032 M, the basic ratio at 3, and the reducing ratio at 14. At 90 °C, the nitrogen disengagement, indicating the decomposition of hydrazine, begins, and the suspension turns black, typically within five minutes. After about two hours, cobalt fibers with a narrow-sized and -shaped distribution, ultrafine dimensions around 0.3−0.4 μm in diameter and 10−40 μm in length, were collected (Figure 3a). When fixing the temperature at 78 °C (sample Co_6), appearance of the gray precipitate, indicating the nucleation of cobalt, was observed after 3 h, and the solution was still dark purple, which indicates that the reaction was not completely finished. The reaction was allowed to proceed for 5 h so that reduction is achieved. The diameter of the cobalt fibers obtained is about 3 μm, and they can be up to 100 μm in length (Figure 3b). The morphology of these fibers is quite different: in the first case, fibers appear to be formed of disks of uniform thickness that coalesce in the direction of the applied magnetic field, whereas they can be considered as formed from aggregation of nanometric particles in the second case. This change in diameter and surface morphology of the fibers might be due to the fact that when the reaction rate decreases (at $T = 78$ °C) the reaction time is prolonged, so the cobalt nucleation proceeds slightly, and the formed particles have the necessary time to agglomerate. Conversely, when the reaction temperature is

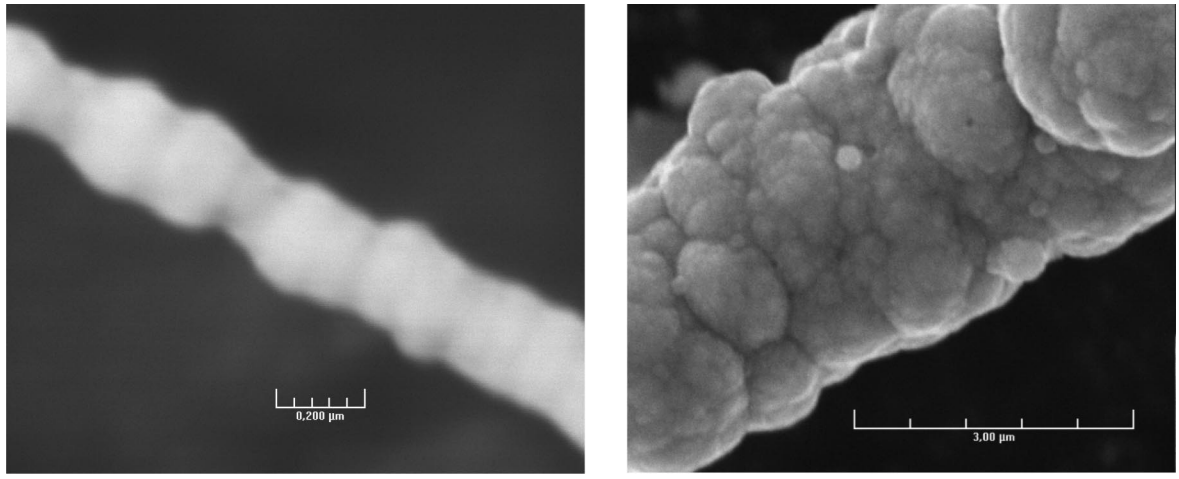

Figure 3. SEM micrographs of cobalt fibers obtained at a reaction temperature of 90 °C (a) and 78 °C (b).

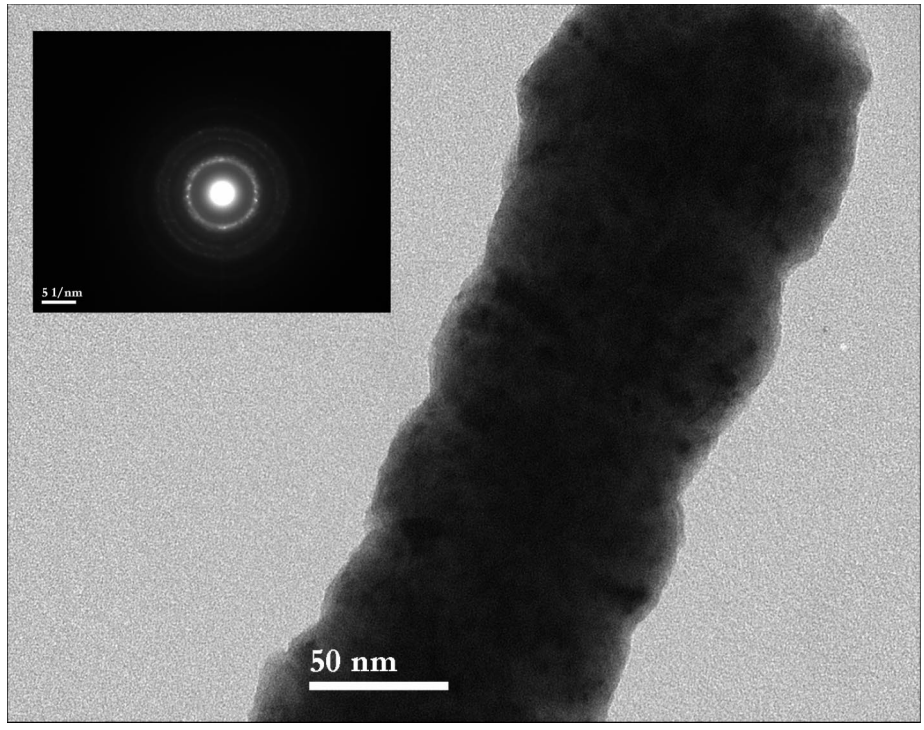

Figure 4. TEM and SAED (inset) micrographs of cobalt fiber obtained in the presence of a nucleating agent, indicating their polycrystalline character.

relatively high (90 °C), the nucleation occurs rapidly, resulting in monodispersed fiber size.

3.3. Effect of the Nucleating Agent. Heterogeneous nucleation using an easy reducible metal has been earlier adopted by Toneguzzo et al.[17] to control the particles size and distribution. In our study, the use of a nucleating agent such as K_2PtCl_4 enables us to elaborate cobalt fibers with uniformly about 0.13 μm in diameter and up to 100 μm in length when the K_2PtCl_4/Co molar ratio is about 2.5×10^{-4} while the other experimental conditions are kept the same as those of sample Co_3. Figure 4 shows a TEM image of an individual Co fiber 125 nm in diameter. The inset of this image is a SAED pattern recorded on this fiber and revealing its polycrystalline character.

3.4. Thermal Analysis. The thermo-gravimetric analysis (TGA) of the as-synthesized submicrometric Co fibers has been performed from room temperature to 973 K (Figure 5) under argon atmosphere. It reveals a total weight loss of 3% between 450 and 750 K that could be attributed to the progressive degradation of the polyol molecules adsorbed on the surface of

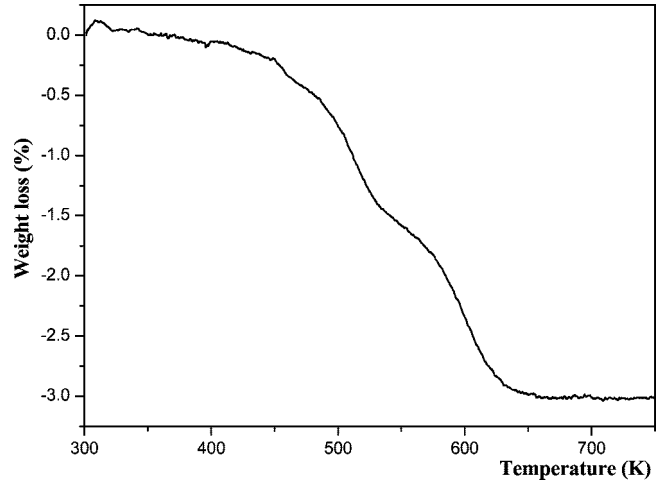

Figure 5. TGA results of dried cobalt fibers.

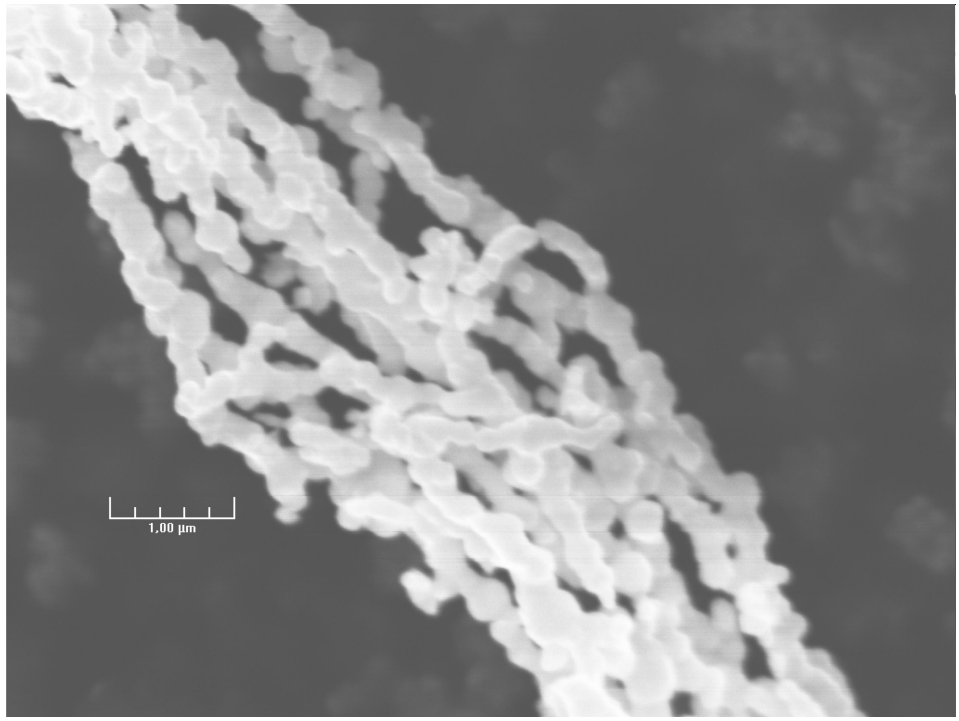

Figure 6. SEM images for the final Co fiber after TGA treatment up to 973 K.

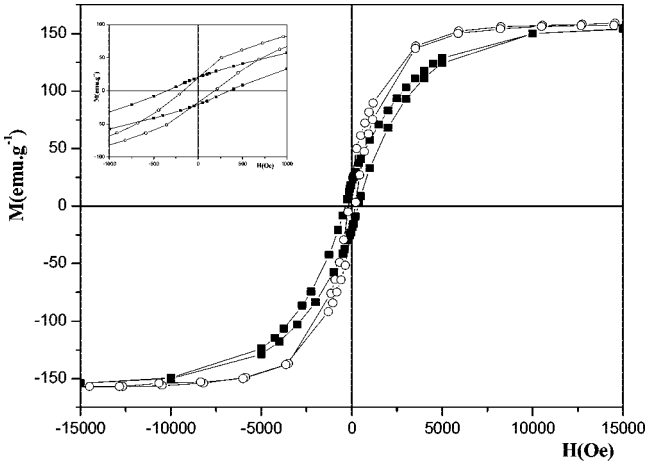

Figure 7. Hysteresis measurements at 5 (−■−) and 300 K (−○−) of submicrometric Co fibers. The inset shows an aggrandizement of the central region.

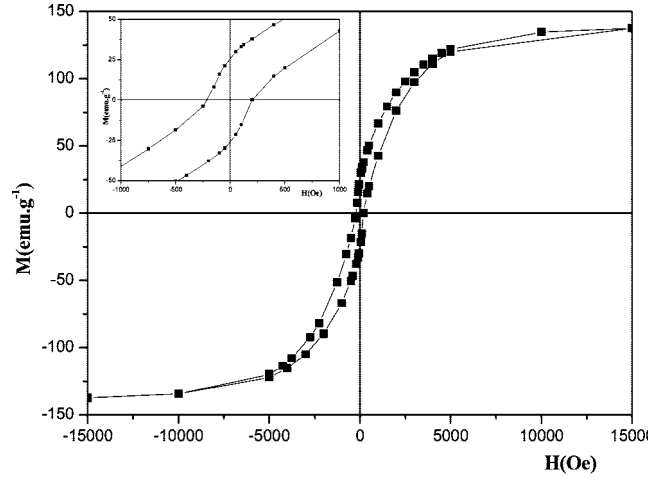

Figure 8. Hysteresis measurements at 5 K of micrometric Co fibers.

the fibers. Thus, the polyol molecules could not be absolutely removed by the wash and the centrifugation procedures. The SEM pattern of the powder after TG treatment (Figure 6) shows that the fibers preserve their morphology up to 973 K with slight increase in diameter and a beginning of fiber coalescence.

3.5. Magnetic Properties of Cobalt Fibers. The magnetic measurements were carried out on the micrometric (D $\approx$ 3 μm) and submicrometric (D $\approx$ 0.13 μm) cobalt fibers. Hysteresis loops of the randomly oriented submicrometric fibers show a ferromagnetic behavior at 5 and 300 K (Figure 7) with coercivities (H_c) of 350 Oe and 162 Oe, respectively. The hysteresis loop recorded on the micrometric fibers at 5 K also illustrates their ferromagnetic behavior (H_c of 222 Oe) (Figure 8). The room-temperature coercivity of the submicrometric fibers is about 46% smaller than the respective value at 5 K, which indicates the important effect of thermal fluctuations on the magnetic behavior of the fibers. Moreover, comparison of coercivity of the submicrometric fibers at 300 K with that of the micrometric fibers at the same temperature shows the significant decrease of coercivity as the fiber increases in diameter. In comparison with bulk Co, which exhibits a coercive field of some tens of oersteds,[18] the coercivities of the as-synthesized fibers are much higher, which could be attributed to their anisotropy as a consequence of both their shape and crystalline structure. However, this enhancement of the magnetic properties of the as-prepared fibers is still small in comparison with the great improvement of coercivities ($H_c \approx 8$ kOe) in Co wires smaller in diameter ($D < 50$ nm).[19−22] Viau et al.[21] reported that the monocrystallinity of the wire slight in diameter leads to the elevated value of H_c, whereas Zheng et al.[22] noted that the monotonical increase of H_c as the diameter decreases is related to the thermal fluctuation that becomes slighter for thinner wires. Thus, the moderate coercive field of the as-synthesized Co fibers is expected since their diameter is still large, which facilitates the formation of magnetic multidomain structures and also the degrading of the coercivity.[20,23] The saturation magnetizations (M_s), about 155 emu g^{-1} for submi-

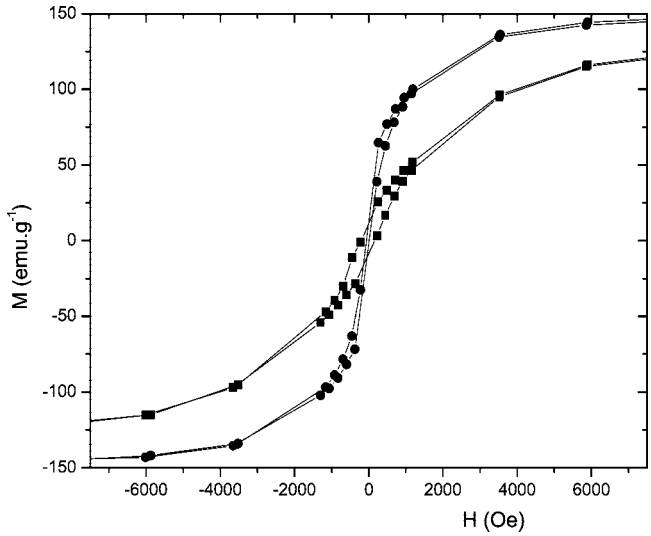

Figure 9. Hysteresis loops at 300 K of cobalt fibers with the magnetic field applied parallel (−●−) and perpendicular (−■−) to the fiber's axis.

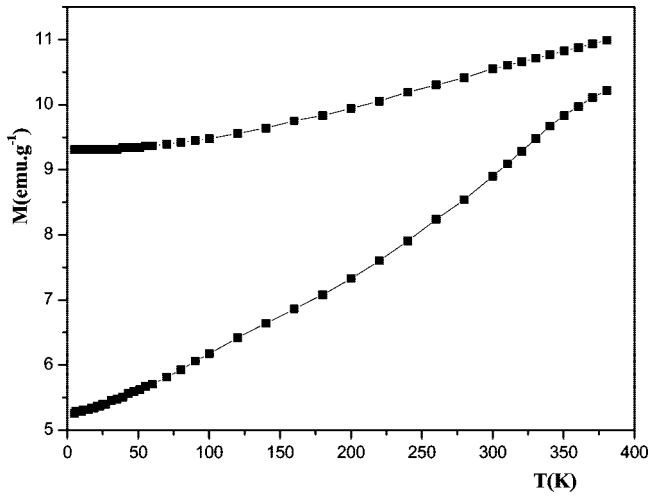

Figure 10. ZFC and FC magnetization curves at $H = 200$ Oe for submicrometric Co fibers.

crometric fibers and 139 emu g^{-1} for micrometric fibers, are reduced relative to the bulk value (168 emu g^{-1}).[24] This fact could be ascribed to the surface oxidation of the grain boundaries or to the presence of polyol molecules adsorbed on the surface of the fibers. Indeed, polyol molecules could quench the magnetic moment through the exchange of electrons between the ligand and the surface of Co atoms, which would partially result in the reduction of saturation magnetization.[18] The TGA analysis of Co fibers confirms the presence of a slight amount of polyol molecules located on the surface of the fibers. Moreover, the hysteresis loops, especially that of submicrometric fibers measured at 300 K, are not symmetric with respect to *x*- and *y*-axes. A very small loop shift is observed. This small loop shift indicates the existence of a slight quantity of antiferromagnetic species on the surface of the fibers, thus implying the exchange bias between ferromagnetic and antiferromagnetic components producing the magnetization shift and the decrease in saturation magnetization.[25−27]

Magnetic measurements on the submicrometric fibers previously oriented parallel and perpendicular to the direction of the magnetic applied field have also been conducted at 300 K. The H_c increases from 30 to 180 Oe when the applied magnetic field was oriented, respectively, parallel and perpendicular to the long axis of the as-synthesized cobalt fibers (Figure 9). Similar results have previously been obtained for cobalt nanowires larger than 40 nm in diameter[9,20,22] and have been ascribed to the fact that the hexagonal *c*-axis is oriented close to the direction perpendicular to the fibers' axis. The X-ray diffraction pattern of as-prepared cobalt fibers (Figure 2b) shows a large increase in the (002) peak's relative intensity in comparison with literature[28] ($((I_{(002)}/I_{(101)})_{obs} \approx 2.14$; $((I_{(002)}/I_{(101)})_{th} \approx 0.6$), which implies that the as-synthesized fibers are highly ordered along the (002) plate and that the hexagonal *c*-axis is effectively oriented perpendicular to the fibers' axis.

The temperature-dependent magnetization of the submicrometric and micrometric Co fibers was measured in ZFC and FC processes at an applied magnetic field of 200 Oe. Figure 10 shows the ZFC/FC magnetization curves of the submicrometric fibers. A large thermal irreversibility is observed, and a very wide energy-barrier distribution can be deduced from the continuous increase in the magnetization in the ZFC curve. As shown by TEM observations (Figure 4), the fibers are formed by self-assembled particles in a privileged direction imposed by the applied field. Each particle appears as a disk 130 nm in diameter and 100 nm high. These dimensions are not sufficiently small to ensure a monodomaine state. However, it seems that for small applied fields, the orientation of the hcp *c*-axis closely perpendicular to the long axis of the fibers favors the split of

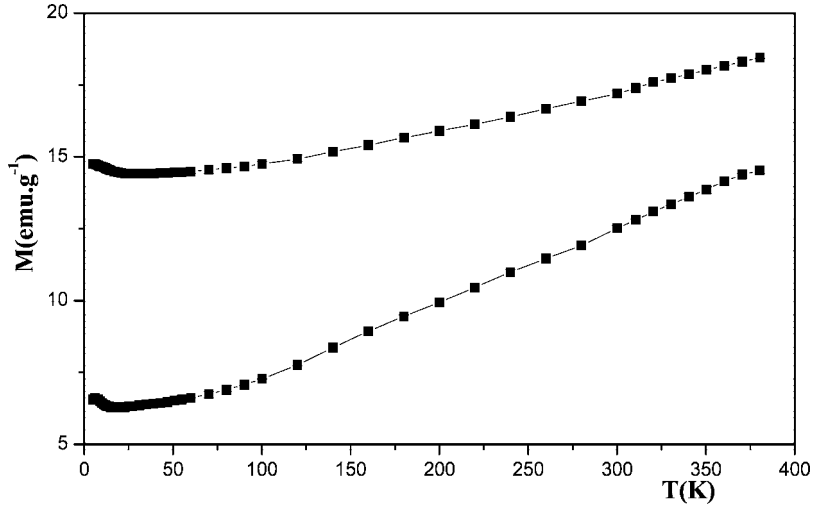

Figure 11. ZFC and FC magnetization curves at $H = 200$ Oe for micrometric Co fibers.

the fibers' magnetization into domains partially oriented perpendicular to the fibers' axis.[22] So, as the temperature increases, the thermal agitation increases, which causes the domain-walls' depinning and thus the gradual increase in the magnetization. As for the micrometric fibers, the ZFC curve (Figure 11) rapidly increases with temperature below 6 K and linearly between 17 and 380 K, which can be attributed to different mechanisms of magnetic alignment. The well-pronounced peak around 6 K can be ascribed to some small Co particles with a volume distribution whose blocking temperatures are around 6 K. From this measured T_B, it is possible to estimate the particles' size using the relation $K_aV = 25k_BT_B$ where K_B is the boltzman constant, and K_aV is the anisotropy energy barrier.[29] Thus, the upper volume of these small particles can be estimated at 1.7 nm using an anisotropy constant of 4.1×10^5 J m^{-3}, calculated for Co nanotubes with $R = 90$ nm and $H = 60$ μm.[30] This result is consistent with the aggregation process proposed to explain the growth mechanism of these micrometric fibers. Over 17 K, the linear increase in magnetization with temperature can be mainly originated from the depinning of domain walls in the multidomain particles.

For micrometric as for submicrometric fibers, the FC magnetizations show a steady drop as the temperature decreases, which is indicative of a strong dipolar magnetostatic interaction between fibers. This behavior has already been observed in strongly interacting particles.[28]

4. Conclusion

A simple method to synthesize cobalt fibers 0.13 μm in average diameter and with an exclusively hcp structure via controlling synthesis parameters is reported. A great enhancement of the magnetic properties of the as-prepared fibers compared to that of the bulk Co has been observed. Magnetic measurements carried out on fibers oriented parallel and perpendicular to the direction of the applied magnetic field shows that they exhibit a ferromagnetic behavior with different saturation magnetization and coercivity in two directions. Two types of temperature dependence of the magnetization have been found in the ZFC curve for the micrometric and submicrometric fibers. The magnetization behavior can be interpreted in terms of the unblocking of the magnetization of the small single domain particles and the depinning of the large multidomain particles in the micrometric fibers and in terms of the depinning of domain walls in multidomain particles in the submcirometric ones.

Acknowledgment. A.D. greatly appreciates the partial financial supports of the Institut Français de Coopération in Tunisia and the Agence Universitaire de la Froncophonie. We also thank Dr. O. Rouleau and Dr. L. Bessais from Laboratoire de Chimie Métallurgique des Terres Rares for the magnetic measurements and for the fruitful discussions about magnetic results and J. Morrice-Abrioux from IUT saint-Denis for the careful reading of the manuscript.

References and Notes

(1) Zhang, Y. J.; Ma, S.; Li, D.; Wang, Z. H.; Zhang, Z. D. *Mater. Res. Bull.* **2008**, *43*, 1957.
(2) Xie, B.-Q.; Qian, Y.; Zhang, S.; Fu, S.; Yu, W. *Eur. J. Inorg. Chem.* **2006**, 2454.
(3) Salgueiriño-Maceira, V.; Correa-Duarte, M. A.; Farle, M.; López-Quintela, M. A.; Sieradzki, K.; Diaz, R. *Langmuir* **2006**, *22* (4), 1455.
(4) Nam, Ch.; Jang, Y.; Lee, K.-S.; Cho, B. K. *Nanotechnology* **2008**, *19*, 015703.
(5) Jiang, Ch.; Wang, L.; Kuwabara, K. J. *Solid State Chem.* **2007**, *180*, 3146.
(6) Zhu, Lu.-P.; Xiao, H.-M.; Fu, S.-Y. *Eur. J. Inorg. Chem.* **2007**, 3947.
(7) Xie, Q.; Dai, Z.; Huang, W.; Liang, J.; Jiang, C.; Qian, Y. *Nanotechnology* **2005**, *16*, 2958.
(8) Henry, Y.; Ounadjela, K.; Piraux, L.; Dubois, S.; George, J.-M.; Duvail, J.-L. *J. Eur. Phys.* **2001**, *B20*, 35.
(9) Paulus, P. M.; Luis, F.; Kröll, M.; Schmid, G.; de Jongh, L. J. *J. Magn. Magn. Mater.* **2001**, *224*, 180.
(10) Petit, C.; Russier, V.; Pileni, M. P. *J. Phys. Chem.* **2003**, *B107*, 10333.
(11) Cao, H.; Xu, Z.; Sang, H.; Sheng, D.; Tie, C. *Adv. Mater.* **2001**, *13* (2), 121.
(12) Tang, Z.; Kotov, N. A. *Adv. Mater.* **2005**, *17* (8), 951, and references therein.
(13) Wang, F.; Gu, H.; Zhang, Z. *Mater. Res. Bull.* **2003**, *38*, 347.
(14) Wu, M.; He, H.; Zhao, Z.; YaO, X. *J. Phys. D:* **2000**, *33*, 2927.
(15) Fiévet, F.; Lagier, J.-P.; Filglarz, M. *MRS Bull.* **1989**, *14*, 29.
(16) ChakrouneN.; Viau, G.; Ricolleau, Ch.; Fiévet-Vincent, F.; Fiévet, F. *J. Mater. Chem* **2003**, *13*, 312.
(17) Toneguzzo, Ph.; Viau, G.; Acher, O.; Fiévet-Vincent, F.; Fiévet, F. *Adv. Mater. Commun* **1998**, *10*, 1032.
(18) van Leeuwen, D. A.; van Ruitenbeek, J. M.; de Jongh, L. J.; Ceriotti, A.; Pacchioni, G.; Häberlen, O. D.; Rösch, N. *Phys. Rev. Lett.* **1994**, *73*, 1432.
(19) Dumestre, F.; Chaudret, B.; Amiens, C.; Fromen, M. C.; Casanove, M. J.; Renaud, P.; Zurcher, P. *Ang. Chem. Int. Ed.* **2002**, *41* (22), 4286.
(20) Henry, Y.; Ounadjela, K.; Piraux, L.; Dubois, S.; George, J.-M.; Duvail, J.-L. *Eur. Phys. J.* **2001**, *B20*, 35, and references therein.
(21) Ung, D.; Viau, G.; Ricolleau, Ch.; Warmont, F.; Gredin, P.; Fiévet, F. *Adv. Mater.* **2005**, *17* (3), 338.
(22) Zeng, H.; Skomski, R.; Menon, L.; Liu, Y.; Bandyopadhyay, S.; Sellmyer, D. J. *Phy. Rev* **2002**, *B65* (13), 134426.
(23) Leslie-Pelecky, D. L.; Rieke, R. D. *Chem. Mater.* **1996**, *8*, 1770.
(24) Dumpich, G.; Krome, T. P.; Hausmans, B. *J. Magn. Magn. Mater.* **2002**, *248*, 241.
(25) Moradi, H.; Gehring, G. A. *J. Magn. Magn. Mater.* **2003**, *256*, 3.
(26) Mushailova, E. S.; Vasiliev, B. V. *J. Magn. Magn. Mater.* **2004**, *279*, 235.
(27) Krivorotov, Ilya N.; Yan, H.; Dan Dahlberg, E.; Stein, A. *J. Magn. Magn. Mater* **2001**, *226−230*, 1800.
(28) JSPDS Card File No. 5-727.
(29) Caffarena, V. R.; Guimar∼aes, A. P.; Folly, W. S. D.; Silva, E. M.; Capitaneo, J. L. *Mater. Chem. Phys.* **2008**, *107*, 297.
(30) Escrig, J.; Landeros, P.; Altbir, D.; Vogel, E. E. *J. Magn. Magn. Mater.* **2007**, *310*, 2448.

JP804461S